The Affects of Molecular Properties of Motive Gas on Supersonic Ejection

Jungkun Jin* and Sejin Kwon**
Division of Aerospace Engineering, KAIST, Daejeon, Korea 305-701

Sehoon Kim***
Agency for Defense Development, Daejeon, Korea,

Abstract

The motive gas of a supersonic ejector is supplied from different sources depending on the application. The performance of an ejector that is represented by the secondary flow pressure, starting and unstarting pressures heavily depends on the molecular properties of the motive gas. The effects of specific heat ratio of the motive gas were investigated experimentally for an axi-symmetric annular injection type supersonic ejector. Both the starting pressure and unstarting pressure, however, decreased with the increase of the specific heat ratio of the motive gas. It was discovered that the secondary flow pressure increased as the specific heat ratio of the motive gas decreased even if the stagnation pressure of the motive flow was invariant. However, when the motive gas flow nozzle area ratio is large enough for the motive gas to be condensed, different tendency was observed.

Key Word : Ejector, Chemical laser, Condensation

Nomenclature

C_P	: Specific heat at constant pressure
MW	: Molecular weight, g/mol
k	: Specific heat ratio
P_{0P}	: Stagnation pressure of motive gas
P_a	: Ambient pressure
P_S	: Static pressure of secondary flow
P_{st}	: Starting pressure of supersonic ejector
P_{unst}	: Unstarting pressure of supersonic ejector

Introduction

An ejector is a device that entrains a secondary flow into a high speed stream that is generated by expansion of high pressure motive gas [1]. It is frequently used to accelerate the secondary flow to a high speed. As the stagnation pressure increases by ejection, an ejector can be regarded as a pump. As an ejector is a purely flow machinery, it has no moving parts and the construction is simpler than conventional pumping devices as a consequence. Supersonic pumping ejectors have been used for applications ranging from the thrust augmentation for V/STOL aircraft [2-5], rocket

* Ph.D. candidate
** Professor, Division of Aerospace Engineering, KAIST
E-mail : trumpet@kaist.ac.kr Tel : +82-42-350-3721 Fax : +82-42-350-3710
*** Senior researcher

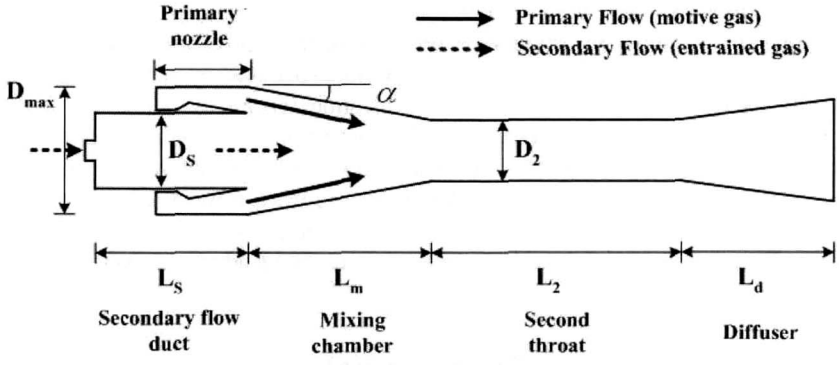

Fig. 1. Geometric configuration of annular injection type supersonic ejector

based combined cycle engine [6] and the high altitude flight environment simulation facility [7, 8] to pumping high power chemical laser [9-11].

Previous researches on the supersonic ejectors largely focused on the geometric design of the ejector system in pursuit of optimum design configuration to meet given requirements. Parametric studies on the effects of the area ratio of the motive gas flow nozzle, the relative areas of motive gas flow nozzle and secondary nozzles and the lengths of the second throat and mixing chamber on the overall ejector performance have been reported [11, 12]. In most of these studies, the motive gas was assumed to be either air or steam with their standard properties.

Studies on the effects on molecular properties on the ejection performance have been rare. As ejectors are incorporated into mobile systems such as high power chemical lasers, the usage of chemical reaction products as a motive gas becomes widespread to allow a compact design. In applications such as ejector-ramjet engine and thrust augmentation for V/STOL aircraft, motive gas flow is supplied by a combustor. As the operating condition of the reactor and combustor varies, the composition of product gas varies as well. Since the driving of an ejector solely depends on the flow interaction, the performance of an ejector is strongly influenced by physical properties of operating gases. Numerous studies have shown that the ejector performance depends on the properties of motive fluid, in particular its average molecular weight [13, 14]. However, properties other than molecular weight of the motive gas also affect the ejection mechanism.

In the present study, we focused on the effects of the specific heat ratio on the performance of supersonic ejector. Experiments were carried out for various gas mixtures with different specific heat ratio. The performances of ejector were estimated in terms of starting pressure, unstarting pressure and the static pressure of secondary flow.

Figure 1 shows the geometric configuration of an annular injection type supersonic ejector used in the present study. Most of the existing ejectors have the motive gas flow injected along the center line of the flow passage of the secondary flow. In applications such as high power chemical lasers, however, annular injection of the motive gas at the periphery of the flow passage is desired to avoid the exposure of the motive gas flow nozzle to the high temperature combustion product gas [6-9]. When supersonic ejector is applied to chemical laser system, secondary flow pressure and mass flow rate are important. Large mass flow rate with low static pressure is required to obtain high power chemical laser. For example, 50 kW level HF-DF chemical laser requires about 500 g/s of secondary flow, and required static pressure of secondary flow is less than 50 torr. In this case, stagnation pressure of secondary flow is 1 ~ 1.5 atm. In the chemical laser application, subsonic secondary flow is entrained by supersonic flow that exhausted from the motive gas flow nozzle, and these two flows are mixed in the mixing chamber. The mixed flow is supersonic flow, and is decelerated in the second-throat by oblique shock waves. The flow exhausted from diffuser is subsonic.

A performance of supersonic ejector can be analyzed on a performance curve [11]. The performance curve can be obtained by measuring the static pressure of the secondary flow at different stagnation

pressures of the motive gas flow while maintaining the secondary mass flow rate fixed. In order to operate the supersonic ejector, the stagnation pressure of the motive gas flow, P_{0P} must be higher than P_{st}. Once the ejector is started, the supersonic operation persists, even when P_{0P} decreases down to a pressure that is less than P_{st}. The supersonic ejection terminates when the P_{0P} is decreased to P_{unst} that is minimum stagnation pressure of the motive gas flow for ejection.

With a fixed mass flow rate of the secondary flow and a constant pressure at the exit of the ejector, the static pressure of the secondary flow pressure, P_S as a function of a stagnation pressure of the motive gas flow indicates the overall performance of the ejector system. Once the ejector is started, the static pressure of the secondary flow is relatively steady but lowest near the unstarting point.

Experimental

For the experiments, two different ejectors were used. Dimensions of the two ejectors are listed Table 1. Two ejectors are mainly different in the motive gas flow nozzle ratio and the diameter of second-throat. Between ejector 1 and ejector 2, only area ratio of motive flow nozzle is different. Ejector 2 and ejector 3 have same motive flow nozzle with different second-throat diameter.

To select the motive gas for the experiments, we assume that the supersonic ejection process can be simulated through ideal gas dynamic calculation. Therefore, it is also assumed that the effect of viscosity is not important in the performance prediction. This assumption can be partially justified by earlier theoretical model proposed by Emanuel [15] that accurately predicted the performance of an ejector of central injection with a similar gas dynamic calculation. With the ideal gas dynamic assumptions, the molecular properties that affect the ejection are condensed to the average molecular weight, the specific heat of the gas at constant pressure and the specific heat ratio. Figure 2 shows the secondary flow pressure predicted through the Emanuel's approach for ejector 1. For the calculation, the stagnation pressure of motive gas flow was assumed to be 15 bar. For the secondary flow, 1 g/s of air was assumed. In Fig. 2, it is noticed that the specific heat ratio is most dominant physical parameter of gas affecting the secondary flow pressure. Therefore, we selected three different gases as a motive gas based on the specific heat ratio for the experiments. The gases used in the experiments are listed in Table 2 including their properties. For ejector 3, the mixture of nitrogen and argon was additionally used as a motive gas. When the mixture of nitrogen and argon was used as the motive gas, they were supplied from separate bottles as non-mixed gases at the same pressure. The specific heats ratio of mixed gas was calculated and it was 1.51.

Table 1. Ejector geometric configurations

Geometry		Ejector 1	Ejector 2	Ejector 3
Area ratio of motive flow nozzle	A_P/A_{P^*}	10.78	3.18	3.18
Diameter of second-throat, mm	D_2	28	28	33
Second-throat L/D ratio	L_2/D_2		8	
Diameter of secondary flow duct, mm	D_S		17	
Outer diameter of the motive flow nozzle exit, mm	D_{max}		44	
Diameter of the diffuser exit, mm	D_d		50	
Contraction angle of the mixing chamber, °	α		4	
Diverging angle of the diffuser, °	β		5	

Table 2. Ejector geometric configurations

Gas	MW, kg/kmol	C_P, J/(kg·K)	k
Argon (Ar)	39.95	521	1.67
Nitrogen (N_2)	28	1006	1.4
Carbon dioxide (CO_2)	44.01	840	1.3

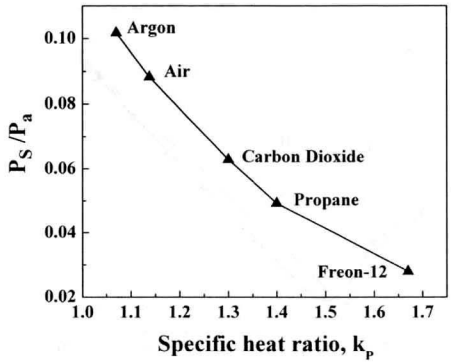

Fig. 2. P_S predicted using Emanuel's approach (P0P = 15 bar, ms = 1 g/s)

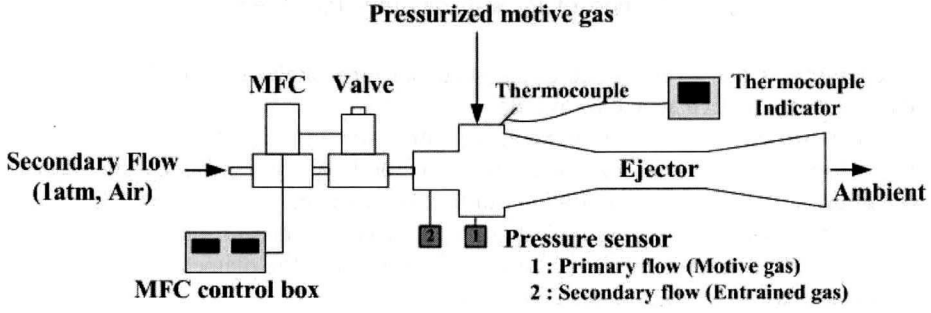

Fig. 3. Experimental setup

Figure 3 is the schematic of the experimental setup. The secondary flow was taken from the ambient air and the flow rate, m_s, was controlled by an MFC (Mass Flow Controller). For each experiment, four different secondary mass flow rates, namely, 0, 1, 2, and 3 g/s were tested. The motive gas flow was supplied from a manifold that was connected to six cylinders of high pressure gases. Since the saturation pressure of carbon dioxide at the room temperature is about 57 bar, some of carbon dioxide can be liquefied in the gas cylinder. If this cylinder is used in the experiment, liquid particles of carbon dioxide can be supplied to the motive gas flow nozzle. To prevent such an unexpected supplement of the liquid particles of carbon dioxide, the mass of carbon dioxide in the cylinder was carefully controlled to minimize the mass of liquefied carbon dioxide in the cylinder before the experiments. The stagnation pressure of motive gas flow and the static pressure of the secondary flow were measured by piezoelectric pressure transducers from the moment of the opening of the valve.

P_{0P} was slowly increased by gradual opening of the valve from the gas manifold. Once the ejector was started, the valve was gradually closed and P_{0P} decreased until the supersonic operation of the ejector was terminated. Using the pressure transition data obtained in this procedure, the performance curve of the ejector that illustrated P_{st}, P_{unst} and P_S were determined.

Results and Discussions

Operation of supersonic ejector

Figure 4 illustrates variation of the secondary flow pressure with different stagnation pressure of motive gas with ejector 2 and argon. In the region A, ejector 2 operated as subsonic ejector. When the stagnation pressure of the motive gas was higher than a certain value, secondary flow pressure increased as the stagnation pressure of the motive gas increased, and the ejector could not operate with supersonic ejecting mode; second-throat and diffuser played roles of throat and diverging section of conventional converging-diverging nozzle. Similar tendency was observed with

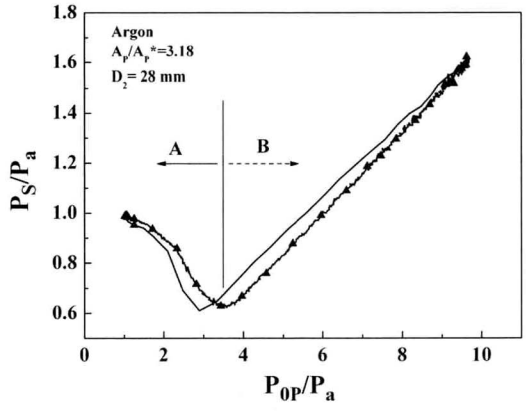

Fig. 4. Change of P_S with different P_{0P} (Ejector 2)

air. This phenomena is due to the small cross-sectional area of the second-throat compared with the throat area of the motive gas flow nozzle.

Figure 5 shows the secondary flow pressure with different stagnation pressure of motive gas with ejector 1. Ejector 3 shows similar result with ejector 1. Arrows indicates the variation of P_{0P} with respect to time. P_S suddenly decreased at starting pressure and suddenly increased at unstarting pressure. The curve shown in Fig. 5 is typical curve of supersonic ejector. Difference between ejector 2 and ejector 3 is only diameter of second-throat. By increasing the diameter of the second-throat, ejector can operate with supersonic ejection mode.

Starting pressure and unstarting pressure

Figure 6 illustrates the starting pressures, P_{st}, and unstarting pressure, P_{unst}, for all three gases as a function of the specific heats ratio when the secondary mass flow rate was 2 g/s. Dashed lines in Fig. 6 indicate estimated value obtained by the normal shock theory [8] for each ejector. P_{st} and P_{unst} shows qualitatively similar behavior with respect to the specific heat ratio of motive gas between both ejectors. As the specific heat ratio of motive gas flow, k_P, increased, both pressures, P_{st} and P_{uns} increased as well.

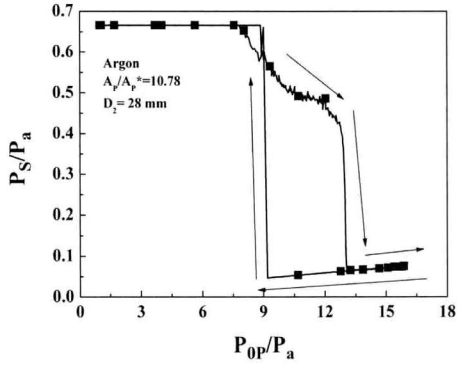

Fig. 5. Change of P_S with different P_{0P} (Ejector 1)

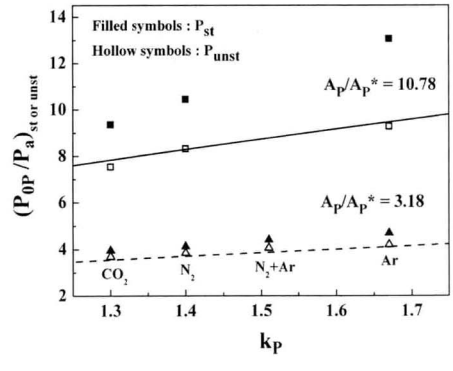

Fig. 6. P_{st} and P_{unst} for ejector 1 and 3. Solid line is predicted value for ejector 1 and dashed line is estimated values for ejector 3 using the normal shock theory for each ejector [14] (m_S = 2 g/s)

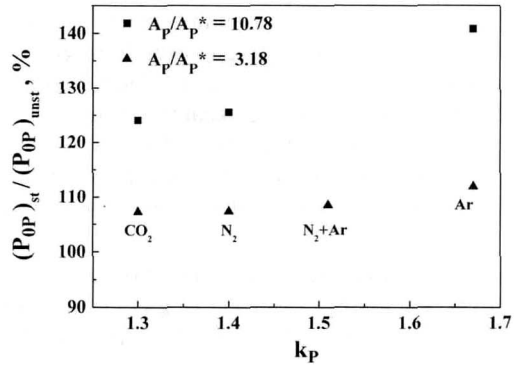

Fig. 7. P_{st}/P_{unst} for Ejector 1 and 3 with different motive gases (m_S = 2 g/s)

The measurement implies that the higher stagnation pressure for the motive gas flow was required in order to start the supersonic ejector when the specific heats ratio was higher. The unstarting pressure measured in the experiments and predicted by the normal shock theory shows a good agreement in Fig. 6. This result is consistent with that of Kim et al [11]. The normal shock theory can estimate the unstarting pressure of the annular injection supersonic ejector regardless of geometric configuration and the properties of the motive gas.

Figure 7 shows the ratio of starting pressure to unstarting pressure. The ratios increased slightly as the k_P increased. When carbon dioxide is used with ejector 3 (A_P/A_P^* = 3.18), the required motive gas pressure to operate ejector is about 107 % of the predicted P_{unst} by normal shock theory. However, in the case of argon, about 112 % of the predicted P_{unst} is required. These ratios increased when the motive gas flow nozzle area ratio increased and the cross-section area of the second-throat decreased (ejector 1).

Secondary flow pressure

The static pressures of the secondary flow that were obtained from the experiments for ejector 1 are illustrated in Fig. 8. All data were obtained for 10.24 bar of the stagnation pressure of the motive gas flow, P_{0P}. The static pressure of the secondary flow that resulted from argon as the motive gas flow was higher by 1 torr than that resulted from air as the motive gas flow with the same stagnation pressure of the motive gas flow in the measurement regardless of the mass flow rates of the secondary flow. This result contradicted what was predicted by the theoretical calculation (Fig. 2), in both of which the static pressure of secondary flow should be higher when the motive gas flow was air with k_P = 1.4. The reason for this discrepancy was due to the condensation of gases at the exit of the motive gas flow nozzle.

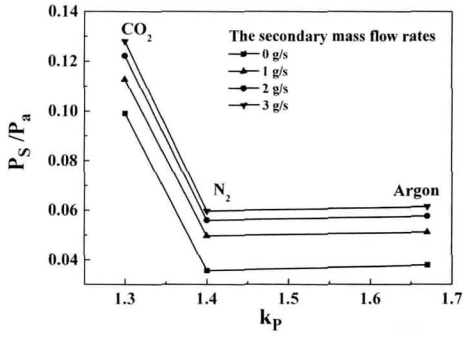

Fig. 8. P_S as a function of specific heat ratio (Ejector 1)

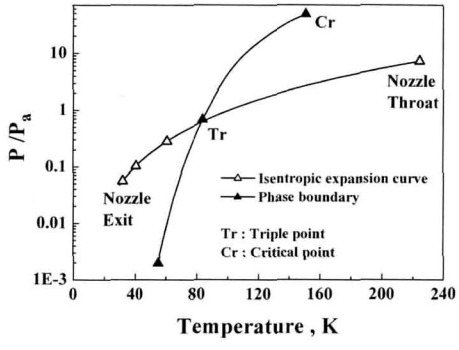

Fig. 9. Phase boundary of argon and isentropic expansion curve in the motive gas flow nozzle (Ejector 1)

The theoretical prediction was made with an assumption that the working fluid was gaseous throughout the passage. Figure 9 shows the phase change curve from gas to liquid and the isentropic expansion process in the motive gas flow nozzle when the working fluid was argon gas on the P-T property plane [16]. When the motive gas was isentropically expanded in the nozzle of the motive gas flow, the state that would have been reached at the end of the nozzle was found in the liquid region. This implies that the assumption of gas phase in the numerical simulation as well as theoretical prediction throughout the ejection process was not valid for certain combination of gas and operating conditions [17, 18].

The condensation phenomenon that complicated observation of the effect of gas properties on ejection performance was due to the excessive expansion of gas in the motive gas flow nozzle with higher area ratio. Therefore, the condensation can be avoided when a smaller area ratio of the motive gas flow nozzle was used.

Figure 10 represents the phase change curve and the isentropic expansion process in a nozzle that had a smaller area ratio at 3.18. The end state of the expansion process through this nozzle of smaller area ratio lied within the region of gas phase, as expansion of the motive gas was not as great as the nozzle with larger area ratio as in Fig. 9. In this case, condensation did not occur and the assumption for the calculation was valid.

The static pressures of the secondary flow, P_S, are plotted in Fig. 11. The curve with square symbols represents the static pressure of the secondary flow when the stagnation pressure of the motive gas flow was 4.4 bar. The static pressure of the secondary flow, P_S, decreased with the specific heats ratio, k, of the motive gas. That tendency is expected results according to the theoretical approach.

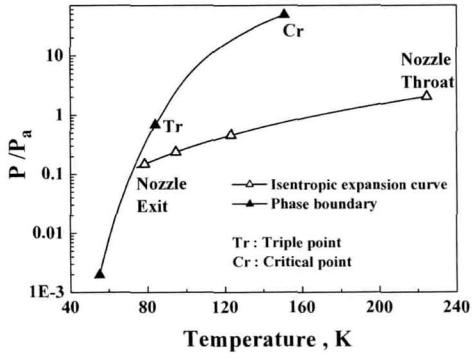

Fig. 10. Phase boundary of argon and isentropic expansion curve in the motive gas flow nozzle (Ejector 3)

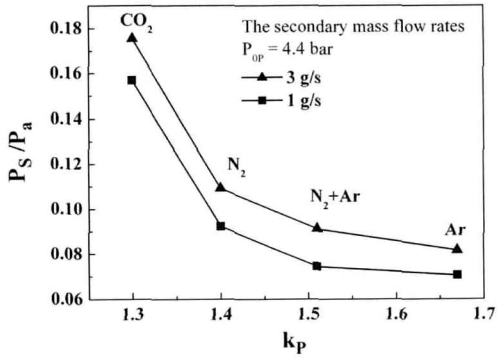

Fig. 11. P_S for different operating gases at 4.4 bar of P_{0P} (Ejector 3)

Conclusions

The effects of the specific heat ratio of the motive gas, k on the performance of the supersonic ejection were investigated for an annular injection type ejector that were typical for a high power chemical laser. The tested performance parameters of the ejector included the starting and unstarting stagnation pressures of the motive gases and the static pressure of the secondary flow. This investigation was essential to correlate the measurement data with a certain gas to arbitrary combustion products that depended on particular application of the ejector.

If there was no condensation of the motive gas flow in the motive gas flow nozzle, the effects of the average molecular weight and specific heat for constant pressure of the motive gas on P_{st}, P_{unst} and P_S were significant and the effects were indirectly expressed in terms of the molar specific heat for constant pressure, $C_{P,mol}$, and specific heat ratio, k, of the motive gas. When the specific heats ratio, k, had low value, P_{st} and P_{unst} were low. However, the static pressure of the secondary flow was relatively high when k of the motive gas was low. The opposite was true for a gas with higher value of k. The starting and unstarting pressures were relatively high but a lower static pressure was possible when k was large.

When the total enthalpy of the motive gas was not sufficiently high, partial condensation occurred at the diverging section of the motive gas flow nozzle. For this case, the numerical simulation as well as theoretical prediction of the ejector performance was not possible. When condensation of motive gas occurred, the static pressure of the secondary flow did not decrease even with a motive gas with large value of k. This is because the condensation of motive gas decreased the ejection capability of the motive gas flow. The measured static pressure of the secondary flow was greater than that of the calculation of non-condensing motive gas. However, P_{st} and P_{unst} were not affected as much as P_S was by the condensation phenomena.

Finally, starting of an annular injection type supersonic was achieved at lower pressure with motive gas that had larger value of k. The starting was expedited when the motive gas flow did not experience condensation within the diverging section of the motive gas flow nozzle.

Acknowledgement

This work was supported by the Korea Science and Engineering Foundation(KOSEF) grant funded by the Korea government (MEST) (No. R01-2006-0000-11311-0)

References

1. Sun, D. W., and Eames, I. W., 1995, "Recent developments in the design theories and applications of ejectors - a review," *Journal of the Institute of Energy*, Vol. 68, pp. 65-79

2. Alperin, M. and Wu, J. J., 1983, "Thrust augmenting ejector, Part I.," *AIAA Journal*, Vol. 21, No. 10, pp. 1428-1436

3. Alperin, M. and Wu, J. J., 1983, "Thrust augmenting ejector, Part II.," *AIAA Journal*, Vol. 21, No. 12, pp. 1698-1706

4. T. G. Tillman and W. M. Presz Jr., 1995, "Thrust Characteristics of a Supersonic Mixer Ejector," *Journal of Propulsion and Power*, Vol. 11, No.5, pp. 931-937

5. Wendy S. Barankiewicz, Gail P. Perusek and Mounir B. Ibrahim, 1994, "Approximate Similarity Principle for a Full-Scale STOVL Ejector," *Journal of Propulsion and Power*, Vol. 10, No. 2, pp. 198-203

6. Takeshi Kanda and Kenji Kudo, 2002, "A Conceptual Study of a Combined Cycle Engine for an Aerospace Plane," *AIAA paper 2002-5146.*

7. Geothert, B. H., 1962, "High altitude and space simulation testing," *ARS Journal*, Vol. 32, No. 12, pp. 872-882

8. Annamalai, K., Visvanathan, K., Sriramulu, V., and Bhaskaran, K. A., 1998, "Evaluation of the performance of supersonic exhaust diffuser using scaled down models," *Experimental Thermal and Fluid Science*, Vol. 17, pp. 217-229

9. Boreisho, A. S., Khailov,V. M., Malkov, V. M., and Savin, A. V., 2000, "Pressure recovery system for high power gas flow chemical laser," *XIII International symposium on gas flow & Chemical lasers - High power laser conference*, International Society for Optical Engineering, Bellingham, WA, pp. 401-405

10. Malkov, V. M., Boreisho, A. S., Savin, A. V., Kiselev, I. A., and Orlov, A. E., 2000, "Choice of working parameters of pressure recovery systems for high-power gas flow chemical lasers," *XIII International symposium on gas flow & Chemical lasers - High power laser conference*, International Society for Optical Engineering, Bellingham, WA, pp. 419-422

11. Sehoon Kim and Sejin Kwon, 2006, "Experimental Determination of Geometric Parameters for an Annular Injection Type Supersonic Ejector," *Journal of Fluid Engineering*, Vol. 28, pp. 1164-1171

12. Dutton, J. C., Mikkelsen, C. D., and Addy, A. L., 1982, "A theoretical and experimental investigation of the constant area, supersonic-supersonic ejector," *AIAA Journal*, Vol. 20, No. 10, pp. 1392-1400

13. Work, L. T. and Haedrich, V. W., H.T., 1939, "Performance of Ejectors as a Function of the Molecular Weights of Vapors," *Industrial and Engineering Chemistry*, Vol. 31, No. 4, pp. 464-477

14. Sam Han, John Peddieson, Jr. and David Gregory, 2002, "Ejector Primary Flow Molecular Weight Effects in an Ejector-Ram Rocket Engine," *Journal of Propulsion and Power*, Vol. 1, No. 3, pp. 592-599

15. Emanuel, G., 1976, "Optimum Performance for a Single-Stage Gaseous Ejector," *AIAA Journal*, Vol. 14, No. 9, pp. 1292-1296

16. Yunus A. Çengel and Michael A. Boles, 1998, *Thermodynamics, An Engineering Approach, 3rd ed.*, McGraw-Hill, International Edition

17. Willmarth, W.W. and Nagamatsu, H.T., 1952, "The Condensation of Nitrogen in Hypersonic nozzle", Journal of Applied Physics, Vol. 23, No. 10, pp. 1089-1095

18. Daum, F. L., 1963, "Air Condensation in a Hypersonic Wind Tunnel," *AIAA Journal*, Vol. 1, No. 5, pp. 1043-1046